

# A Three-Step Approach for Assessing Landscape Connectivity via Simulated Dispersal: African Wild Dog Case Study

David D. Hofmann<sup>1,2,§</sup>  Gabriele Cozzi<sup>1,2</sup>  John W. McNutt<sup>2</sup>  
Arpat Ozgul<sup>1</sup>  Dominik M. Behr<sup>1,2</sup> 

November 17, 2022

<sup>1</sup> Department of Evolutionary Biology and Environmental Studies, University of Zurich,  
Winterthurerstrasse 190, 8057 Zurich, Switzerland.

<sup>2</sup> Botswana Predator Conservation Program, Private Bag 13, Maun, Botswana.

§ Corresponding author (david.hofmann2@uzh.ch)

**Running Title:** Simulating Wild Dog Dispersal Trajectories to Assess Landscape  
Connectivity

**Keywords:** dispersal, simulation, movement, integrated step-selection function,  
Kavango-Zambezi Transfrontier Conservation Area, landscape connectivity, *Lycaon pictus*

## Abstract

**Context** Dispersal of individuals contributes to long-term population persistence, yet requires a sufficient degree of landscape connectivity. To date, connectivity has mainly been investigated using least-cost analysis and circuit theory, two methods that make assumptions that are hardly applicable to dispersal. While these assumptions can be relaxed by explicitly simulating dispersal trajectories across the landscape, a unified approach for such simulations is lacking.

**Objectives** Here, we propose and apply a simple three-step approach to simulate dispersal and to assess connectivity using empirical GPS movement data and a set of habitat covariates.

**Methods** In step one of the proposed approach, we use integrated step-selection functions to fit a mechanistic movement model describing habitat and movement preferences of dispersing individuals. In step two, we apply the parameterized model to simulate dispersal across the study area. In step three, we derive three complementary connectivity maps; a heatmap highlighting frequently traversed areas, a betweenness map pinpointing dispersal corridors, and a map of inter-patch connectivity indicating the presence and intensity of functional links between habitat patches. We demonstrate the applicability of the proposed three-step approach in a case study in which we use GPS data collected on dispersing African wild dogs (*Lycaon pictus*) inhabiting northern Botswana.

**Results** Using step-selection functions we successfully parametrized a detailed dispersal model that described dispersing individuals' habitat and movement preferences, as well as potential interactions among the two. The model substantially outperformed a model that omitted such interactions and enabled us to simulate 80,000 dispersal trajectories across the study area.

**Conclusion** By explicitly simulating dispersal trajectories, our approach not only requires fewer unrealistic assumptions about dispersal, but also permits the calculation of multiple connectivity metrics that together provide a comprehensive view of landscape connectivity. In our case study, the three derived connectivity maps revealed several wild dog dispersal hotspots and corridors across the extent of our study area. Each map highlighted a different aspect of landscape connectivity, thus emphasizing their complementary nature. Overall, our case study demonstrates that a simulation-based approach offers a simple yet powerful alternative to traditional connectivity modeling techniques. It is therefore useful for a variety of applications in ecological, evolutionary, and conservation research.

# **1 Introduction**

2 Dispersal of individuals is a vital process that allows species to maintain genetic diversity  
3 (Perrin and Mazalov, 2000; Frankham et al., 2002; Leigh et al., 2012; Baguette et al., 2013;  
4 LaPoint et al., 2013), rescue non-viable populations (Brown and Kodric-Brown, 1977), and  
5 to colonize unoccupied habitats (Hanski, 1999; MacArthur and Wilson, 2001). However, the  
6 ability to disperse depends on a sufficient degree of landscape connectivity (Fahrig, 2003;  
7 Clobert et al., 2012), making the identification and protection of dispersal corridors that  
8 promote connectivity a task of fundamental importance (Doerr et al., 2011; Rudnick et al.,  
9 2012). Identifying dispersal corridors not only necessitates a comprehensive understanding  
10 of the factors that limit dispersal, but also an appropriate model to estimate connectivity  
11 (Baguette et al., 2013; Vasudev et al., 2015; Hofmann et al., 2021a). To date, the most  
12 commonly used connectivity models are least-cost path analysis (LCPA; Adriaensen et al.,  
13 2003) and circuit theory (CT; McRae, 2006; McRae et al., 2008). Unfortunately, both models  
14 rest on assumptions that appear unsuitable for dispersers, thus calling for the development  
15 of alternative approaches. One promising alternative is to assess landscape connectivity via  
16 simulated dispersal trajectories generated from individual-based movement models (IBMMs,  
17 Diniz et al., 2019). However, IBMMs require a large number of subjective modeling decisions,  
18 thus making among-system comparisons difficult.

19 Traditional connectivity models make assumptions that are rarely met for dispersers.  
20 LCPA, for instance, assumes that individuals move towards a preconceived endpoint and  
21 choose a cost-minimizing route accordingly (Sawyer et al., 2011; Abrahms et al., 2017).  
22 While this assumption may be justifiable for migrating animals, it is unlikely to hold for  
23 dispersers, as dispersers typically move across unfamiliar territory towards an unknown end-  
24 point (Koen et al., 2014; Cozzi et al., 2020). CT, on the contrary, posits that animals move  
25 according to a random walk, entailing that autocorrelation between subsequent movements  
26 cannot be rendered (Diniz et al., 2019). For dispersers, however, autocorrelated movements  
27 are regularly observed (Cozzi et al., 2020; Hofmann et al., 2021a), meaning that dispersal  
28 trajectories are usually strongly directional. An interesting generalization that bridges the  
29 continuum between LCPA and CT has been proposed by (Panzacchi et al., 2016) and enables  
30 to capitalize on the merits of both approaches. Despite these and several other generaliza-  
31 tions of LCPA and CT (e.g. Pinto and Keitt, 2009; Landguth et al., 2012; Panzacchi et al.,  
32 2016; Brennan et al., 2020), some shortcomings remain. Most notably, all of these methods  
33 rely on static permeability or resistance surfaces that can't reflect the temporal dimension of  
34 dispersal. This permits statements about the expected duration for moving between habitat

35 patches (Martensen et al., 2017; Diniz et al., 2019).

36 The shortcomings inherent to LCPA and CT can be overcome by simulating dispersal  
37 using IBMMs and by converting simulated trajectories into meaningful measures of connec-  
38 tivity (Diniz et al., 2019). In contrast to LCPA and CT, IBMMs allow to explicitly simulate  
39 how individuals move across and interact with the encountered landscape (Kanagaraj et al.,  
40 2013; Clark et al., 2015; Allen et al., 2016; Hauenstein et al., 2019; Zeller et al., 2020), as  
41 well as to render potential interactions between movement behavior and habitat conditions  
42 (Avgar et al., 2016). This shifts the focus towards a more functional view on connectivity  
43 (Tischendorf and Fahrig, 2000). Furthermore, IBMMs generate movement sequentially, i.e.  
44 they generate a series of steps, so that the temporal dimension of dispersal becomes explicit  
45 and allows modeling autocorrelation between successive steps (Diniz et al., 2019). Finally,  
46 simulations from IBMMs do not enforce movement or connections towards preconceived  
47 endpoints but allow individuals to adjust their route “on the go”, thereby preventing biases  
48 arising from misplaced endpoints. Despite these advantages, a unifying approach to simu-  
49 late dispersal and assess connectivity using IBMMs is lacking. Considering the large number  
50 of subjective decisions entailed by IBMMs, an approach that streamlines and standardizes  
51 the application of dispersal simulations to assess connectivity will, however, be critical to  
52 safeguard comparability among studies.

53 Here, we propose and exemplify a simple three-step approach for simulating dispersal and  
54 assessing landscape connectivity (Figure 1). In step one, we combine GPS movement data  
55 of dispersing individuals with habitat covariates to fit a mechanistic movement model via in-  
56 tegrated step-selection functions (ISSFs, Avgar et al., 2016). We chose to use ISSFs because  
57 the framework not only allows inference on the study species’ habitat kernel (i.e. its habi-  
58 tat preferences), but also its movement kernel (i.e. its movement preferences/capabilities)  
59 and potential interactions among the two (Avgar et al., 2016; Fieberg et al., 2021). In  
60 step two, we use the parametrized movement model to simulate dispersal across the study  
61 area. Comparable simulations have already been applied to estimate steady-state utilization  
62 distributions of resident individuals (Potts et al., 2013; Signer et al., 2017) and to model  
63 landscape connectivity, yet disregarding interdependencies between habitat and movement  
64 kernels (Clark et al., 2015; Zeller et al., 2020). Finally, in step three, we convert the simulated  
65 trajectories into three complementary connectivity maps; (i) a heatmap revealing frequently  
66 traversed areas (e.g. Hauenstein et al., 2019; Zeller et al., 2020), (ii) a betweenness-map  
67 delineating dispersal corridors and bottlenecks (e.g. Bastille-Rousseau et al., 2018), (iii) and  
68 a map of inter-patch connectivity, depicting the presence and intensity of functional links

69 between habitat patches, as well as the average dispersal duration required to realize those  
70 connections (e.g. Gustafson and Gardner, 1996; Kanagaraj et al., 2013).

71 We showcase the application of the proposed approach using GPS movement data col-  
72 lected on dispersing African wild dogs (*Lycaon pictus*). The African wild dog is a highly  
73 mobile species whose population persistence heavily relies on the availability of large, natural  
74 or semi-natural landscapes and a sufficient degree of connectivity among remaining subpop-  
75 ulations. Once common throughout sub-Saharan Africa, this species has disappeared from  
76 much of its historic range, largely due to human persecution, habitat fragmentation, and  
77 disease outbreaks (Woodroffe and Sillero-Zubiri, 2012). Wild dogs typically disperse in  
78 single-sex coalitions (McNutt, 1996; Behr et al., 2020) and are capable of dispersing several  
79 hundred kilometers (Davies-Mostert et al., 2012; Masenga et al., 2016; Cozzi et al., 2020).  
80 Although previous studies have investigated connectivity for this species using LCPA (Hof-  
81 mann et al., 2021a) and CT (Brennan et al., 2020), a more comprehensive and mechanistic  
82 understanding of dispersal and connectivity is missing (but see Creel et al., 2020). Nev-  
83 ertheless, with about 6,000 free-ranging wild dogs remaining in fragmented subpopulations  
84 (Woodroffe and Sillero-Zubiri, 2012), reliable information on dispersal behavior and land-  
85 scape connectivity is essential for the conservation of this endangered carnivore. We antic-  
86 ipated that a connectivity assessment based upon our three-step approach would overcome  
87 several of the conceptual shortcomings of traditional connectivity models, while providing  
88 a more detailed view on movement behavior during dispersal its implications for landscape  
89 connectivity.

## 90 **2 Methods**

### 91 **2.1 Case Study**

#### 92 **2.1.1 GPS Data**

93 We applied the three step approach presented in Figure 1 to GPS movement data from  
94 16 dispersing African wild dog coalitions (7 female and 9 male coalitions). This data has  
95 been collected between 2011 and 2019 from a free-ranging wild dog population in northern  
96 Botswana. During dispersal, GPS collars recorded a fix every 4 hours and regularly trans-  
97 mitted data over the Iridium satellite system. To ensure comparable time intervals between  
98 GPS fixes, we removed any fixes that were not successfully obtained at the desired 4-hour  
99 schedule (allowing for a tolerance of  $\pm$  15 minutes). To prepare the data for step-selection  
100 analysis, we converted the fixes ( $n = 4'169$ ) into steps, where each step represented the

101 straight-line movement between two consecutive GPS fixes (Turchin, 1998). We only con-  
102 sidered steps with equal step-durations (i.e. 4 hours) for further analysis. We will refer to  
103 these steps as “realized steps”. We did not differentiate between sexes, for previous research  
104 found little differences between sexes during dispersal (Woodroffe et al., 2019; Cozzi et al.,  
105 2020). Additional details on the data collection and preparation can be found in Cozzi et al.  
106 (2020) and Hofmann et al. (2021a).

### 107 **2.1.2 Study Area**

108 Our simulation of dispersal trajectories and assessment of connectivity spanned across the  
109 entire Kavango-Zambezi Transfrontier Conservation Area (KAZA-TFCA, Figure 2a and b)  
110 and encompassed a rectangular extent of roughly 1.3 Mio. km<sup>2</sup>. With an area of 520'000  
111 km<sup>2</sup>, the KAZA-TFCA is the world’s largest transboundary conservation area and comprises  
112 parts of Angola, Botswana, Namibia, Zimbabwe, and Zambia, thus hosting a rich diversity  
113 of landscapes, ranging from savannah to grassland and from dry to moist woodland habitats.  
114 In its center lies the Okavango Delta, a dominant hydro-geographical feature and the world’s  
115 largest flood-pulsing inland delta. Large portions of the KAZA-TFCA are formally protected  
116 in the form of national parks (NPs) or other protected areas, yet a considerable portion of  
117 the landscape remains human-dominated (e.g. roads, agricultural sites, and settlements).

### 118 **2.1.3 Habitat Covariates**

119 We represented the physical landscape in our study area by the habitat covariates `water-`  
120 `cover`, `distance-to-water`, `woodland-cover`, `shrub/grassland-cover`, and `human-influence`. To  
121 render the seasonal dynamics of water-cover for the extent of the Okavango Delta, we  
122 applied an algorithm that enabled us to obtain weekly updated raster-layers for `water-`  
123 `cover` and `distance-to-water` from MODIS satellite imagery (Wolski et al., 2017; Hofmann  
124 et al., 2021a). This algorithm is now implemented in the `floodmapr` package (available on  
125 GitHub; <https://github.com/DavidDHofmann/floodmapr>). To ensure a consistent resolu-  
126 tion across habitat covariates, we coarsened or interpolated all layers to a resolution of 250  
127 m x 250 m. A detailed description of how we prepared each habitat covariate is provided in  
128 Hofmann et al. (2021a).

129 We performed all data preparations, spatial computations, and statistical analysis in  
130 R, version 3.6.6 (R Core Team, 2020). Some helper functions were written in C++ and  
131 imported into R using the Rcpp package (Eddelbuettel and François, 2011; Eddelbuettel,  
132 2013; Eddelbuettel and Balamuta, 2018).

<sup>133</sup> **2.2 Step 1 - Movement Model**

<sup>134</sup> We combined the collected GPS data with habitat covariates and used ISSFs (Avgar et al.,  
<sup>135</sup> 2016) to parametrize a mechanistic movement model. More specifically, we paired each  
<sup>136</sup> realized step with a set of 24 randomly generated alternative steps. A realized and its 24  
<sup>137</sup> random steps together formed a stratum that received a unique identifier. As suggested by  
<sup>138</sup> Avgar et al. (2016), we generated random steps by sampling random turning angles from a  
<sup>139</sup> uniform distribution  $(-\pi, +\pi)$  and step lengths from a gamma distribution that was fitted  
<sup>140</sup> to realized steps (scale  $\theta = 6'308$  and shape  $k = 0.37$ ). Note that our approach of sampling  
<sup>141</sup> turning angles from a uniform distribution does not imply that we assume uniform turning  
<sup>142</sup> angles, as we will account for directionality later in the model (Avgar et al., 2016; Fieberg  
<sup>143</sup> et al., 2021).

<sup>144</sup> Along each realized and random step, we extracted values from underlying habitat covari-  
<sup>145</sup> ate layers and we computed averages of each covariate along the steps. Besides extracting  
<sup>146</sup> *habitat covariates*, we also computed movement metrics that we used as *movement covari-  
147 ates* in the ISSF models (Avgar et al., 2016; Fieberg et al., 2021). Specifically, we computed  
<sup>148</sup> the step length (`sl`), its natural logarithm (`log(sl)`), and the cosine of the relative turning  
<sup>149</sup> angle (`cos(ta)`), which is a measure of directionality (Turchin, 1998), for each step. Because  
<sup>150</sup> wild dog activity is low during the hot midday hours (Cozzi et al., 2012), we additionally  
<sup>151</sup> created the variable `LowActivity`, indicating whether a step was realized during periods of  
<sup>152</sup> low wild dog activity (09:00 to 17:00 local time) or high wild dog activity (17:00 to 09:00  
<sup>153</sup> local time). To facilitate model convergence, we standardized all continuous covariates to  
<sup>154</sup> a mean of zero and a standard deviation of one. Correlations among covariates were low  
<sup>155</sup> ( $|r| < 0.6$ ; Latham et al., 2011), so we retained all of them for modeling.

<sup>156</sup> To contrast realized steps (scored 1) and random steps (scored 0), we assumed that  
<sup>157</sup> animals assigned a selection score  $w(x)$  to each step (Equation 1; Fortin et al., 2005), where  
<sup>158</sup>  $w(x)$  depended on the step's associated covariates  $(x_1, x_2, \dots, x_n)$  and on the animal's relative  
<sup>159</sup> selection strengths (Avgar et al., 2017) towards these covariates  $(\beta_1, \beta_2, \dots, \beta_n)$ :

$$w(x) = \exp(\beta_1 x_1 + \beta_2 x_2 + \dots + \beta_n x_n) \quad (\text{Equation 1})$$

<sup>160</sup> The probability of a step  $i$  being realized was then contingent on the step's selection score,  
<sup>161</sup> as well as on the selection scores of all other step in the same stratum:

$$P(Y_i = 1 | Y_1 + Y_2 + \dots + Y_i = 1) = \frac{w(x_i)}{w(x_1) + w(x_2) + \dots + w(x_i)} \quad (\text{Equation 2})$$

162 To estimate relative selection strengths (i.e. the  $\beta$ -coefficients), we used mixed effects  
163 conditional logistic regression analysis, implemented through the r-package `glmmTMB` (Brooks  
164 et al., 2017). The implementation of conditional logistic regression has been proposed by  
165 Muff et al. (2020) and allows to model random slopes. The method requires to fix the vari-  
166 ance of the stratum specific intercept to a large value, so we fixed it to an arbitrary high  
167 value of  $10^6$  and used disperser identity to model random slopes for all covariates.

168 Our movement model was based on a habitat selection model that was previously devel-  
169 oped for dispersing wild dogs (hereafter referred to as *base model*, Hofmann et al., 2021a).  
170 In the base model, no interactions among habitat covariates and movement covariates were  
171 considered, so we here expanded the model and allowed for such interactions, acknowledging  
172 that movement preferences during dispersal could depend on habitat conditions (details in  
173 Appendix A1). To determine the most parsimonious movement model among model can-  
174 didates, we ran stepwise forward model selection based on Akaike's Information Criterion  
175 (AIC, Burnham and Anderson, 2002). More specifically, we started with the base model  
176 and iteratively increased model complexity by adding all possible interactions between move-  
177 ment and habitat covariates. Given that the focus of our analysis lied on predicting dispersal  
178 patterns and all model candidates were biologically intuitive, we deemed the use of model  
179 selection appropriate. However, caution should be employed if causal relationships are of  
180 interest, as model selection may lead to biased parameter estimate (Whittingham et al.,  
181 2006). We validated the predictive power of the most parsimonious model using k-fold  
182 cross-validation for case-control studies as described in Fortin et al. (2009). This valida-  
183 tion attests significant prediction ability to the movement model if the model outperforms a  
184 random guess and systematically assigns low ranks (high selection scores) to observed steps  
185 (details in Appendix A2).

### 186 2.3 Step 2 - Dispersal Simulation

187 We used the most parsimonious movement model to simulate individual dispersal trajectories  
188 across the study area. The simulation of a dispersal trajectory resembled an “inverted”  
189 ISSF and was set up as follows. (1) We defined a source point and assumed a random initial  
190 orientation of the simulated animal. (2) Starting from the source point, we generated 25  
191 random steps by sampling turning angles from a uniform distribution  $(-\pi, +\pi)$  and step  
192 lengths from our fitted gamma distribution. (3) Along each random step, we extracted and  
193 averaged values from the habitat covariate layers and we computed the movement metrics  
194  $sl$ ,  $\log(sl)$ , and  $\cos(ta)$ . To ensure compatible scales with the fitted movement model, we

195 standardized covariate values using means and standard deviations from the empirical data.  
196 (4) We applied the parametrized movement model to predict the selection score  $w(x)$  for each  
197 step using Equation 1 and we converted predicted scores into probabilities using Equation 2.  
198 (5) We randomly sampled one of the generated random steps based on assigned probabilities  
199 and determined the animal's new position. We repeated steps (2) to (5) until 2,000 steps  
200 were realized and we repeated the simulation until a total of 80'000 dispersal trajectories  
201 was reached.

202 As source points for the simulations, we distributed 50,000 points at random locations  
203 inside protected areas that were large enough to host an average size wild dog home range  
204 (i.e. > 700 km<sup>2</sup>; Pomilia et al., 2015). We placed another 30,000 points randomly inside the  
205 buffer zone, mimicking potential immigration into the study area (Figure S1).

206 To mitigate edge effects and to deal with random steps leaving the study area, we followed  
207 Koen et al. (2010) and artificially expanded all covariate layers by a 100 km wide buffer  
208 zone. Within the buffer zone, we randomized covariate values by resampling values from the  
209 original covariate layers. Through this buffer zone, simulated dispersers were able to leave  
210 and re-enter the main study area. In cases where random steps crossed the outer border of  
211 this buffer zone, we resampled steps until they fully lied within the buffer zone, essentially  
212 forcing simulated individuals to remain within the expanded study area.

213 To ensure reliable connectivity estimates, we determined the number of simulated dis-  
214 persal trajectories required to reach a “steady state”. For this purpose, we distributed 1,000  
215 rectangular “checkpoints”, each with an arbitrary extent of 5 km x 5 km, at random co-  
216 ordinates within the study area (excluding the buffer). We then determined the relative  
217 frequency at which each checkpoint was traversed by simulated dispersal trajectories (here-  
218 after referred to as relative traversal frequency) as we gradually increased the number of  
219 simulated trajectories from 1 to 50,000. To assess variability in the relative traversal fre-  
220 quency, we repeatedly subsampled 100 times from all 50'000 trajectories and computed the  
221 mean traversal frequency across replicates, as well as its 95% prediction-interval for each  
222 checkpoint. We considered connectivity to have reached a steady state once the width of  
223 the prediction-interval dropped below a value of 0.01 for all checkpoints.

## 224 **2.4 Step 3 - Connectivity Maps**

### 225 **2.4.1 Heatmap**

226 To identify dispersal hotspots within the study area, we created a heatmap indicating the  
227 absolute frequency at which different areas were traversed by simulated dispersal trajectories

(e.g. Hauenstein et al., 2019; Zeller et al., 2020). Specifically, we rasterized all simulated trajectories onto a raster with 1 km x 1 km resolution and tallied resulting layers into a single map. This procedure ensured that every trajectory was only counted once, even if it traversed the same raster-cell multiple times, thus reducing potential biases caused by individuals that were surrounded by unfavorable habitat and “moved in circles”. To achieve high performance rasterization, we used the R-package `terra` (Hijmans, 2021).

#### 2.4.2 Betweenness Map

To pinpoint movement corridors and bottlenecks, we converted simulated trajectories into a network and calculated betweenness scores for all raster-cells in the study area (Bastille-Rousseau et al., 2018). Betweenness is a pertinent metric for connectivity as it measures how often a specific network-node (in our case a raster-cell) lies on a shortest path between any other pair of nodes (Bastille-Rousseau et al., 2018). To convert simulated trajectories into a network, we followed Bastille-Rousseau et al. (2018) and overlaid the study area (including the buffer) with a raster containing 2.5 km x 2.5 km raster-cells, where the center of each raster-cell served as node in the final network. To identify edges (i.e. connections) between the nodes, we used the simulated trajectories and determined all transitions occurring from one cell to another, as well as the frequency at which those transitions occurred (see also Appendix A4). This resulted in an edge-list that we translated into a weighted network using the r-package `igraph` (Csardi and Nepusz, 2006). The final weight of each edge was determined by the frequency of transitions, yet because `igraph` handles edge weights ( $\omega$ ) as costs, we inverted the traversal-frequency through each raster-cell by applying  $\omega = \frac{\text{mean}(\text{TraversalFrequency})}{\text{TraversalFrequency}_i}$ . Consequently, regularly used edges received small weights (i.e. low costs) and vice versa. We used the weighted network to calculate betweenness scores for all network nodes.

#### 2.4.3 Inter-Patch Connectivity Map

To examine the presence and intensity of functional links (i.e. connections) between patches within the study area, we calculated inter-patch connectivity (e.g. Gustafson and Gardner, 1996, Kanagaraj et al., 2013). For this, we computed the relative frequency at which dispersers originating from one patch successfully moved into another patch. We considered movements between patches as successful if an individual’s dispersal trajectory originating from the source patch intersected with the target patch at least once. For each trajectory we also recorded the number of steps required to reach the first intersection with the respective

patch, allowing us to compute the average dispersal durations from one patch to another. In summary, we determined *if* and *how often* dispersers moved between certain patches, as well as *how long* individuals had to move to make these connections. In our case study, we used NPs as patches to determine inter-patch connectivity, hence we'll use the terms interchangeably from here on. The decision to focus on NPs was purely out of simplicity and should not imply that dispersal between other areas is impossible.

#### 2.4.4 Validation

To validate our predictions of connectivity, we utilized additional dispersal data that was collected on eight dispersing coalitions between the years 2019 and 2022 (totalling to 2'668 GPS locations). We used path selection analysis (PSF, Cushman and Lewis, 2010) to assess if observed dispersal trajectories followed areas of high predicted connectivity. Similar to SSF, PSF enables to detect selection for certain features by comparing observed paths to randomly generated paths. Here, we paired each observed path with 50 random paths that we generated by randomly rotating and shifting observed paths by a random angle  $\alpha \sim U(-\pi, +\pi)$  and a random distance  $d \sim U(0 \text{ km}, 50 \text{ km})$ . Along each path, we then extracted connectivity values from the heatmap (see above) generated after 68, 125, 250, 500, and 2'000 simulated steps, respectively. Finally, we ran conditional logistic regression to contrast observed and random paths. In case of systematic selection for high-connectivity areas, the regression coefficients from the corresponding conditional logistic regression model should be positive.

## 3 Results

The most parsimonious movement model consisted of movement covariates, habitat covariates, as well as several of their interactions, thus suggesting that movement behavior during dispersal depended on habitat conditions (Figure 3a, Table S1 and Table S2). Although multiple models received an AIC weight  $> 0$  (Table S1), we only considered results from the most parsimonious model for simplicity. This decision only marginally influenced subsequent steps as all models with positive AIC weights retained similar covariates (Table S1). The k-fold cross-validation showed that the final model substantially outperformed a random guess and provided reliable predictions (i.e. confidence intervals of  $\bar{r}_{s,realized}$  and  $\bar{r}_{s,random}$  did not overlap). Moreover, the model correctly assigned high selection scores to realized steps (Figure 3b), indicating a good fit between predictions and observations. As can be taken from the Spearman rank correlation coefficient, the inclusion of several

interactions between movement and habitat covariates significantly improved model performance ( $\bar{r}_{s,realized} = -0.65$ ; 95% – CI = [-0.67, -0.64]), compared to the base model ( $\bar{r}_{s,realized} = -0.55$ ; 95% – CI = [-0.57, -0.52]; Hofmann et al., 2021a). Our validation of the resulting connectivity maps using independent dispersal data showed that dispersers preferentially followed areas of high predicted connectivity, as coefficients from the PSF models were all significantly greater than zero (Figure 3c). The movement model thus successfully predicted functional connectivity.

Plots that aid with the interpretation of the most parsimonious movement model are provided in Figure S3 and suggest that, under average conditions, dispersing wild dogs avoided moving through water, woodlands, and areas dominated by humans, but preferred moving across shrublands or grasslands (Figure 3a). Dispersers realized shorter steps (indicating slower movements) in areas covered by water or woodland, while realizing larger steps in areas dominated by shrubs or grass (Figure 3a). We found a particularly large effect for the variable **LowActivity**, suggesting that dispersing wild dogs moved substantially faster during twilight and at night (i.e. between 17:00 and 09:00 o'clock; Figure 3a). Although dispersers revealed a preference for directional movements (i.e. low turning angles), especially when moving quickly, they did less so in proximity to humans or water, resulting in more tortuous movements in such areas (Figure 3a).

### 3.1 Dispersal Simulation

Dispersal simulations based on the most parsimonious movement model proved useful for assessing landscape connectivity. Of the 50,000 simulated dispersal trajectories that originated from the main study area, only 4.5% reached a map boundary, suggesting that we successfully mitigated biases from boundary effects. Moreover, our examination of the relative traversal frequency across all checkpoints showed that the relative traversal frequency reached a steady state after 10,500 simulated dispersal trajectories (Figure S4). Although variability in the relative traversal frequency kept decreasing as we increased the number of simulated dispersers, the marginal benefit of simulating additional trajectories diminished quickly (Figure S4).

### 3.2 Heatmap

The heatmap (Figure 4), which resulted from the summation of all simulated dispersal trajectories, allowed us to pinpoint areas that were frequently visited and enabled us to compare areas inside and outside the KAZA-TFCA borders with respect to the intensity at which they

were used for dispersal. For instance, we could deduct that areas inside the KAZA-TFCA were frequently traversed by dispersers (median traversal frequency inside KAZA-TFCA = 166, IQR = 274, Figure S7a), whereas areas beyond the KAZA-TFCA boundary were comparatively rarely visited (median traversal frequency outside KAZA-TFCA = 61, IQR = 133, Figure S7a). Most notably, the region in northern Botswana south of the Linyanti swamp appeared to serve as highly frequented dispersal hotspot (median traversal frequency = 987, IQR = 558). Aside from revealing movement hotspots, the heatmap also provided information on areas that appeared to hinder movement. For example, extensive water bodies, such as the Okavango Delta, the Makgadikgadi Pan, and the Linyanti swamp, substantially restricted dispersal movements and limited realized connectivity inside the KAZA-TFCA. Similarly, the landscapes of Zambia and Zimbabwe were only rarely used for dispersal, even within the KAZA-TFCA boundaries (Figure S8a). Despite the fact that the heatmap improved our understanding of the frequency at which areas were traversed by simulated dispersers, it seemed impractical to pinpoint dispersal corridors.

### 3.3 Betweenness

The betweenness map (Figure 5) revealed several distinct dispersal corridors that run across the study area. In comparison to the heatmap, the betweenness map was less biased towards areas with many dispersers and pronounced narrower, more linear routes that were used by simulated individuals to move between regions. Again, northern Botswana emerged as a wild dog dispersal corridor that connected more remote regions in the study area. Towards east, the extension of this corridor ran through Chobe NP into Hwange NP. From there, a further extension connected to Matusadona NP in Zimbabwe. Northwest of the Linyanti ecosystem, a major corridor expanded into Angola, where it split and finally traversed over a long stretch of unprotected area into Zambia's Kafue NP. Several additional corridors with lower betweenness scores emerged, yet most of them ran within the KAZA-TFCA boundaries (median betweenness inside KAZA-TFCA =  $6.947 \times 10^6$ , IQR =  $54.311 \times 10^6$ , Figure S7b). Consequently, only few corridors directly linked the peripheral regions of the KAZA-TFCA and passed through unprotected areas outside its borders (mean betweenness outside KAZA-TFCA =  $2.685 \times 10^6$ , IQR =  $9.891 \times 10^6$ , Figure S7b).

### 3.4 Inter-Patch Connectivity

The inter-patch connectivity map showed that the relative frequency at which simulated dispersal trajectories moved from one patch to another varied, as did the average dispersal

duration between patches (Figure 6). The map thereby completed the picture on connectivity and provided valuable insights into the frequency and duration of connections between patches. For some patches, we also detected imbalances between the number of incoming and outgoing links, hinting at possible source-sink dynamics. From Chobe NP, for instance, 510 individuals reached the Moremi NP, yet the opposite route was only realized by 340 individuals. Relative to the number of simulated individuals, however, these numbers correspond to fractions of 50% and 68%, respectively. Overall, inter-patch connectivity between patches in Angola, Namibia, Botswana, and Zimbabwe appeared to be high; between 54% and 87% of individuals originating from a patch in these countries successfully moved into at least one other patch (Figure S9a). Conversely, only 19% of the dispersers leaving from a patch in Zambia managed to find their way into some other patch (Figure S9b). Prior to reaching another patch, individuals from Angola, Namibia, Botswana, Zimbabwe, and Zambia had to move for an average of 630, 640, 940, 1045, and 890 steps, respectively. Furthermore, it appeared that the corridor previously identified on Figure 6 between Angola's NPs and the Kafue NP in Zambia is only rarely realized.

## 4 Discussion

Here, we presented a simple three-step approach to assess landscape connectivity via simulated dispersal trajectories and we demonstrated its application using empirical data from a free-ranging population of African wild dogs. In step one, we used ISSFs to parametrize a fully mechanistic movement model describing how individuals move through the landscape. Aside from rendering habitat preferences, the model also encapsulated movement preferences and potential interactions between movement and habitat preferences. In step two, we employed the movement model and simulated dispersal trajectories across the landscape. In comparison to more traditional connectivity modeling techniques, such simulations require fewer unrealistic assumptions about dispersal and enable the derivation of multiple connectivity metrics. Hence, in step three, we translated the simulated trajectories into three complementary connectivity maps, each emphasizing a different aspect of landscape connectivity (e.g. frequently traversed areas, critical dispersal corridors and bottlenecks, and the presence and intensity of functional links between suitable patches).

Results on the habitat kernel from our model showed that dispersers avoided areas dominated by humans and covered by water, but selected for regions with open grassland in the vicinity to water bodies. This largely complied with previous studies that investigated habitat selection by dispersing wild dogs (Davies-Mostert et al., 2012; Masenga et al., 2016;

389 Woodroffe et al., 2019; O'Neill et al., 2020; Hofmann et al., 2021a). However, instead of  
390 merely generating insights on dispersers' habitat preferences, the ISSF framework also per-  
391 mitted us to model several additional complexities common to dispersal. For instance, by  
392 including the interactions  $\cos(\text{ta}):sl$  and  $\cos(\text{ta}):\log(sl)$ , we could accommodate that dis-  
393 persers exhibit turning angles that are correlated with step lengths, meaning that turning  
394 angles tend to be smaller when individuals move fast. Although similar autocorrelations  
395 could be incorporated by sampling step lengths and turning angles from copula probability  
396 distributions (Hodel and Fieberg, 2022), the ISSF framework allowed us to conveniently  
397 model such peculiarities directly in the movement model. While we only considered first  
398 order autocorrelation, i.e. correlation between two consecutive steps, higher order autocor-  
399 relation is conceivable and may be desirable to model (Dray et al., 2010; McClintock et al.,  
400 2012). However, this will require vast amounts of GPS data that are not interrupted by  
401 missing fixes; something that is rarely achieved in reality (Graves and Waller, 2006). The  
402 power and flexibility of ISSFs to model additive effects between habitat and movement co-  
403 variates (Avgar et al., 2016; Signer et al., 2017) furthermore allowed us to formally capture  
404 that dispersing wild dogs move slower and more tortuous in areas covered by water. Such  
405 effects may be of limited interest and novelty from a biological perspective, yet they are  
406 important to be considered when simulating dispersal, in particular if one is interested in  
407 estimating dispersal durations between habitat patches. Overall, the inclusion of interac-  
408 tions between habitat and movement covariates in our movement model lead to a significant  
409 improvement in predictive performance compared to an earlier model that omitted such  
410 interactions (Hofmann et al., 2021a).

411 Each of the three connectivity maps derived from simulated dispersal trajectories high-  
412 lighted a different aspect of landscape connectivity. The heatmap was most suitable for  
413 pinpointing frequently traversed areas and showed that an exceptionally large number of  
414 dispersers moved through the regions of the Moremi NP and the Chobe NP in northern  
415 Botswana. Hofmann et al. (2021a) previously identified the same area as potential dispersal  
416 hotspot using LCPA, however, following their analysis it was not clear whether this was the  
417 consequence of the central location of the region and connections being enforced between  
418 predefined start and endpoints. Contrary to LCPA, a simulation-based approach as pre-  
419 sented here does not require predefined endpoints, as endpoints emerge naturally from the  
420 simulated dispersal trajectories. This is especially useful for dispersal studies, where known  
421 endpoints are usually an unrealistic assumption (Elliot et al., 2014; Abrahms et al., 2017;  
422 Cozzi et al., 2020). The fact that the same region was emphasized using vastly different

423 methods to model connectivity thus reinforces our notion that the area is of exceptional  
424 importance to dispersing wild dogs. Because simulated individuals are not forced to move  
425 towards certain endpoints, a simulation-based approach not only lends itself to study land-  
426 scape connectivity, but also to uncover potential dispersal traps (Van der Meer et al., 2014)  
427 or areas with a high susceptibility for human wildlife conflicts (Cushman et al., 2018).

428 In contrast to the heatmap, the betweenness map emphasized relatively narrow and lin-  
429 ear movement routes. It thus facilitated the identification of discrete movement corridors.  
430 While in some cases both the heatmap and the betweenness map attributed a high im-  
431 portance to the same areas (e.g. northern Botswana), little consensus was found for other  
432 regions. For instance, the stretch of unprotected land between Luengue-Luiana NP in An-  
433 gola and the Kafue NP in Zambia was characterized by a high betweenness-scores, yet it  
434 only received low scores on the heatmap. This is due to the differential way in which the  
435 maps view connectivity. While the heatmap attributes a high connectivity to areas that are  
436 frequently traversed, it does not distinguish between areas that truly bring individuals into  
437 other regions of the study area and regions that lead into ecological traps. The converse is  
438 true on the betweenness map, as it strictly highlights regions that promote movement into  
439 other areas of the landscape and thus promote gene-flow. However, neither of the two maps  
440 provides insights into functional links between distinct habitat patches or how connections  
441 depend on the dispersal duration. For this reason, we also produced a map of inter-patch  
442 connectivity. This map depicted the frequency at which simulated individuals moved be-  
443 tween patches as well as the average dispersal duration (in steps) required to realize them.  
444 Calculating dispersal durations was only possible because trajectories were simulated spa-  
445 tially and temporally explicitly, something that is currently unfeasible with LCPA or CT. An  
446 explicit representation of time enables answerings questions such as: “*How long will it take a*  
447 *disperser to move from A to B?*” or “*Is it possible for a disperser to move from A to B within*  
448 *X days?*”. Moreover, it yields opportunities to incorporate seasonality and to investigate  
449 whether dispersal corridors exist seasonally or all-year round (*dynamic connectivity*; Zeller  
450 et al., 2020). With LCPA or CT, seasonality can currently only be incorporated through  
451 the preparation of multiple permeability surfaces on which the same connectivity model is  
452 repeatedly applied (e.g. Osipova et al., 2019). With simulations from ISSFs, in contrast, the  
453 environment could change “as the dispersers move”, so that simulated trajectories would  
454 dynamically respond to seasonal fluctuations in the environment.

455 Our approach enabled us to translate a simple set of small-scale behavioral rules into large  
456 scale patterns of connectivity, something previously deemed computationally unfeasible, yet

critical for linking structural and functional connectivity (Doerr et al., 2011). Structural connectivity focuses purely on the spatial arrangement of suitable habitat in the landscape, whereas functional connectivity also takes into account a species dispersal ability and behavioral response to the landscape (Tischendorf and Fahrig, 2000). Functional connectivity is of greater interest to conservation scientists, yet is difficult to quantify (Baguette et al., 2013), which is why structural connectivity often serves as surrogate Doerr et al. (2011); Fattebert et al. (2015). LCPA and CT incorporate functional aspects of connectivity through the permeability surface, which reflects a species habitat preferences and thus renders behavioral impacts of the landscape on the focal species. Aside from rendering habitat preferences, our model also integrates peculiarities of the focal species movement behavior, thus adding further insights on functional connectivity. In addition, we could use independent dispersal data to prove that our predictions of connectivity aligned with observed functional connectivity patterns.

Despite the many benefits and great flexibility offered by simulations from ISSFs, one must also be aware of the associated limitations. For example, while our approach of simulating dispersal proved useful to assess landscape connectivity, it was computationally costly. Simulating 80,000 dispersal trajectories for 2'000 steps across the KAZA-TFCA required five days of computation on a regular desktop machine (AMD Ryzen 7 2700X octa-core processor with 3.6 GHz, 64 GB of RAM). The long simulation time was primarily caused by the massive extent of the study area considered (ca. 1.8 Mio km<sup>2</sup>), the large number of simulated trajectories, and the fact that we extracted covariates along each step, rather than just at their start or endpoints. Most connectivity studies focus on smaller study areas (e.g. Kanagaraj et al., 2013; Clark et al., 2015; McClure et al., 2016; Abrahms et al., 2017; Zeller et al., 2020) and will therefore require fewer simulations and achieve faster simulation times (given the same spatial resolution). We also believe that fewer simulated trajectories will often suffice, as the relative traversal frequency by simulated trajectories through randomly placed checkpoints across our study area converged already after 10,500 runs. The exact number of required simulations to achieve reliable estimates of connectivity will, of course, vary depending on the structure of the landscape and the dispersal capabilities of the focal species (Gustafson and Gardner, 1996). For species that disperse short distances through homogeneous environments, few simulations may suffice to gauge connectivity, whereas for species that disperse over long distances through heterogeneous habitats, a large number of simulations will be required to sufficiently explore the spectrum of possible routes. Finally, it may often suffice to extract covariates at each step's start or endpoints, thus considerably

491 speeding up simulation times (Signer et al., 2017).

492 Aside from the computational requirements, simulations further entail several non-trivial  
493 but important modeling decisions. On four such decisions we would like to further elaborate:  
494 (1) the number of simulated individuals, (2) the location of source points, (3) the simulated  
495 dispersal duration, and (4) the behavior at map boundaries.

496 (1) When simulating dispersal trajectories, the modeler needs to decide on the number  
497 of simulated individuals. A higher number is always desirable, as each additional trajectory  
498 provides information about landscape connectivity. However, each additional simulation  
499 imposes computational costs, so a trade-off needs to be managed. Signer et al. (2017)  
500 proposed to handle the trade-off by simulating additional individuals only until the metrics  
501 of interest converge towards a steady state. Here, we used the relative traversal frequency  
502 as target metric and found that it converged already after 10'500 simulated individuals.  
503 The exact number of required individuals might, however, vary depending on the employed  
504 target metric and the anticipated connectivity map. More sophisticated target metrics than  
505 the relative traversal frequency, preferably tailored to different connectivity maps, need to  
506 be developed in the future.

507 (2) To initiate dispersers, a modeler needs to provide a set of source points at which  
508 the virtual dispersers are released. We placed source points within protected areas large  
509 enough to sustain viable wild dog populations, implicitly assuming that wild dogs primarily  
510 survive in large, formally protected areas (Davies-Mostert et al., 2012; Woodroffe and Sillero-  
511 Zubiri, 2012; Van der Meer et al., 2014). Moreover, we lacked precise knowledge about  
512 the distribution and abundance of wild dogs across protected areas, so we placed source  
513 points randomly within them. In cases where more detailed data about the distribution and  
514 abundance of the focal species are available, source points could be distributed accordingly.  
515 Alternatively, source points could be distributed homogeneously but later be weighted when  
516 computing connectivity metrics. In any case, the challenge of selecting meaningful source  
517 points is not unique to individual-based simulations but also applies to LCRA and CT.

518 (3) The use of ISSFs to simulate dispersers requires deciding on the number of simulated  
519 steps (i.e. the simulated dispersal durations). If sufficient dispersal data of the focal species  
520 has been collected, dispersal durations could be sampled from observed dispersal events or  
521 from parametric distributions fit to observed data. Due to the low number of observed  
522 dispersal events, we opted against this solution and instead simulated all individuals for  
523 2,000 steps, which was at the upper end of observed dispersal durations in African wild  
524 dogs (Davies-Mostert et al., 2012; Masenga et al., 2016; Cozzi et al., 2020; Hofmann et al.,

525 2021a). This approach had the advantage that it allowed us to systematically shorten the  
526 simulated trajectories after their simulation and thereby to investigate the sensitivity of our  
527 results with respect to exact dispersal durations (Figures S5 and S6).

528 (4) Unless simulated dispersal trajectories are strongly drawn towards a point of attraction  
529 inside the study area(e.g. Signer et al., 2017), some trajectories will inevitably approach  
530 one of the map boundaries. In this case, one or more of the generated random steps might  
531 leave the study area, making it impossible to compute a selection score. A possible solution  
532 is to simply terminate the simulation of the affected trajectory, assuming that the simulated  
533 individual has left the study area. However, this approach might produce ambiguous results  
534 in cases where many individuals are released near map borders, especially because already a  
535 single random step leaving the study area will break the simulation, thus resulting in biased  
536 connectivity estimates along map borders. Rather than breaking the simulation, we created  
537 a buffer zone (Koen et al., 2010) and resampled random steps until they fully lied within  
538 the study area. This proved to be an effective solution to overcome problems with boundary  
539 effects.

540 In summary, we proposed and applied a simple three-step approach that relies on ISSF-  
541 analysis and enables the simulation of dispersal trajectories and the assessment of landscape  
542 connectivity. The proposed approach overcomes several of the conceptual shortcomings  
543 inherent to LCPA and CT, such as the assumption of known endpoints, and provides a highly  
544 flexible tool for investigating connectivity. Moreover, the simulation of dispersal opens up  
545 new avenues for incorporating interactions between habitat and movement covariates and  
546 provides the foundation for a rich suite of complementary connectivity measures. With  
547 this work, we hope to have sparked interest in the application, optimization, or creation  
548 of methods to investigate dispersal and connectivity via individual-based simulations, while  
549 at the same time stressing some of the non-trivial modeling decisions involved. We also  
550 hope to provide a useful framework that helps unifying and streamlining the application of  
551 individual-based simulations for assessing landscape connectivity.

## 552 5 Authors' Contributions

553 D.D.H., D.M.B., A.O. and G.C. conceived the study and designed methodology; D.M.B.,  
554 G.C., and J.W.M. collected the data; D.D.H. and D.M.B. analysed the data; G.C. and A.O.  
555 assisted with modeling; D.D.H., D.M.B., and G.C. wrote the first draft of the manuscript and  
556 all authors contributed to the drafts at several stages and gave final approval for publication.

## **6 Data Availability**

557 GPS movement data of dispersing wild dogs is available on dryad (Hofmann et al., 2021b).  
558 Access to R-scripts that exemplify the application of the proposed approach using simulated  
559 data are provided through Github (<https://github.com/DavidDHofmann/DispersalSimulation>).  
560 In addition, all codes required to reproduce the African wild dog case study will be made  
561 available through an online repository at the time of publication.  
562

## **7 Acknowledgements**

563 We thank the Ministry of Environment and Tourism of Botswana for granting permission  
564 to conduct this research. We thank C. Botes, I. Clavadetscher, and G. Camenisch for  
565 assisting with wild dog immobilizations. We also thank B. Abrahms for sharing her data  
566 of three dispersing wild dogs. Furthermore, we would like to thank Johannes Signer for  
567 assisting with the simulation algorithm. This study was funded by Albert-Heim Foundation,  
568 Basler Stiftung für Biologische Forschung, Claraz Foundation, Idea Wild, Jacot Foundation,  
569 National Geographic Society, Parrotia Stiftung, Stiftung Temperatio, Wilderness Wildlife  
570 Trust, Forschungskredit of the University of Zürich (grant no. FK-21-091), and a Swiss  
571 National Science Foundation grant (no. 31003A\_182286) to A. Ozgul.  
572

## **8 Conflict of Interest**

573 All authors declare that they have no conflicts of interest.  
574

## 575 References

- 576 Abrahms, B., Sawyer, S. C., Jordan, N. R., McNutt, J. W., Wilson, A. M., and Brashares,  
577 J. S. (2017). Does Wildlife Resource Selection Accurately Inform Corridor Conservation?  
578 *Journal of Applied Ecology*, 54(2):412–422.
- 579 Adriaensen, F., Chardon, J., De Blust, G., Swinnen, E., Villalba, S., Gulinck, H., and  
580 Matthysen, E. (2003). The Application of Least-Cost Modelling as a Functional Landscape  
581 Model. *Landscape and Urban Planning*, 64(4):233–247.
- 582 Allen, C. H., Parrott, L., and Kyle, C. (2016). An Individual-Based Modelling Approach to  
583 Estimate Landscape Connectivity for Bighorn Sheep (*Ovis canadensis*). *PeerJ*, 4:e2001.
- 584 Avgar, T., Lele, S. R., Keim, J. L., and Boyce, M. S. (2017). Relative Selection Strength:  
585 Quantifying Effect Size in Habitat- and Step-Selection Inference. *Ecology and Evolution*,  
586 7(14):5322–5330.
- 587 Avgar, T., Potts, J. R., Lewis, M. A., and Boyce, M. S. (2016). Integrated Step Selection  
588 Analysis: Bridging the Gap Between Resource Selection and Animal Movement. *Methods  
in Ecology and Evolution*, 7(5):619–630.
- 589 Baguette, M., Blanchet, S., Legrand, D., Stevens, V. M., and Turlure, C. (2013). Indi-  
590 vidual Dispersal, Landscape Connectivity and Ecological Networks. *Biological Reviews*,  
591 88(2):310–326.
- 592 Bastille-Rousseau, G., Douglas-Hamilton, I., Blake, S., Northrup, J. M., and Wittemyer,  
593 G. (2018). Applying Network Theory to Animal Movements to Identify Properties of  
594 Landscape Space Use. *Ecological Applications*, 28(3):854–864.
- 595 Behr, D. M., McNutt, J. W., Ozgul, A., and Cozzi, G. (2020). When to Stay and When  
596 to Leave? Proximate Causes of Dispersal in an Endangered Social Carnivore. *Journal of  
597 Animal Ecology*, 89(10):2356–2366.
- 598 Brennan, A., Beytell, P., Aschenborn, O., Du Preez, P., Funston, P., Hanssen, L., Kilian,  
599 J., Stuart-Hill, G., Taylor, R., and Naidoo, R. (2020). Characterizing Multispecies  
600 Connectivity Across a Transfrontier Conservation Landscape. *Journal of Applied Ecology*,  
601 57:1700–1710.
- 602 Brooks, M. E., Kristensen, K., van Benthem, K. J., Magnusson, A., Berg, C. W., Nielsen,  
603 A., Skaug, H. J., Maechler, M., and Bolker, B. M. (2017). glmmTMB Balances Speed and  
604 Flexibility among Packages for Zero-Inflated Generalized Linear Mixed Modeling. *The R  
605 Journal*, 9(2):378–400.
- 606 Brown, J. H. and Kodric-Brown, A. (1977). Turnover Rates in Insular Biogeography: Effect  
607 of Immigration on Extinction. *Ecology*, 58(2):445–449.
- 608 Burnham, K. P. and Anderson, D. R. (2002). *Model Selection and Multimodel Inference: A  
609 Practical Information-Theoretic Approach*. Springer Science & Business Media, Ney York,  
610 NY, USA.
- 611 Clark, J. D., Laufenberg, J. S., Davidson, M., and Murrow, J. L. (2015). Connectivity among  
612 Subpopulations of Louisiana Black Bears as Estimated by a Step Selection Function. *The  
613 Journal of Wildlife Management*, 79(8):1347–1360.
- 614 Clobert, J., Baguette, M., Benton, T. G., and Bullock, J. M. (2012). *Dispersal Ecology and  
615 Evolution*. Oxford University Press, Oxford, UK.
- 616 Cozzi, G., Behr, D. M., Webster, H. S., Claase, M., Bryce, C. M., Modise, B., Mcnutt, J. W.,  
617 and Ozgul, A. (2020). African Wild Dog Dispersal and Implications for Management. *The  
618 Journal of Wildlife Management*, pages 614–621.
- 619 Cozzi, G., Broekhuis, F., McNutt, J. W., Turnbull, L. A., Macdonald, D. W., and Schmid,  
620 B. (2012). Fear of the Dark or Dinner by Moonlight? Reduced Temporal Partitioning  
621 among Africa's Large Carnivores. *Ecology*, 93(12):2590–2599.
- 622

- 623 Creel, S., Merkle, J., Mweetwa, T., Becker, M. S., Mwape, H., Simpamba, T., and  
 624 Simukonda, C. (2020). Hidden Markov Models Reveal a clear Human Footprint on the  
 625 Movements of Highly Mobile African Wild Dogs. *Scientific reports*, 10(1):1–11.
- 626 Csardi, G. and Nepusz, T. (2006). The igraph Software Package for Complex Network  
 627 Research. *InterJournal, Complex Systems*:1695.
- 628 Cushman, S. A., Elliot, N. B., Bauer, D., Kesch, K., Bahaa-el din, L., Bothwell, H., Flyman,  
 629 M., Mtare, G., Macdonald, D. W., and Loveridge, A. J. (2018). Prioritizing Core Areas,  
 630 Corridors and Conflict Hotspots for Lion Conservation in Southern Africa. *PLOS ONE*,  
 631 13(7):e0196213.
- 632 Cushman, S. A. and Lewis, J. S. (2010). Movement Behavior Explains Genetic Differentiation  
 633 in American Black Bears. *Landscape Ecology*, 25(10):1613–1625.
- 634 Davies-Mostert, H. T., Kamler, J. F., Mills, M. G. L., Jackson, C. R., Rasmussen, G. S. A.,  
 635 Groom, R. J., and Macdonald, D. W. (2012). Long-Distance Transboundary Dispersal  
 636 of African Wild Dogs among Protected Areas in Southern Africa. *African Journal of  
 637 Ecology*, 50(4):500–506.
- 638 Diniz, M. F., Cushman, S. A., Machado, R. B., and De Marco Júnior, P. (2019). Landscape  
 639 Connectivity Modeling from the Perspective of Animal Dispersal. *Landscape Ecology*,  
 640 35:41–58.
- 641 Doerr, V. A. J., Barrett, T., and Doerr, E. D. (2011). Connectivity, Dispersal Behaviour  
 642 and Conservation under Climate Change: A Response to Hodgson et al.: Connectivity  
 643 and Dispersal Behaviour. *Journal of Applied Ecology*, 48(1):143–147.
- 644 Dray, S., Royer-Carenzi, M., and Calenge, C. (2010). The Exploratory Analysis of Autocor-  
 645 relation in Animal-Movement Studies. *Ecological Research*, 25(3):673–681.
- 646 Eddelbuettel, D. (2013). *Seamless R and C++ Integration with Rcpp*. Springer, New York.  
 647 ISBN 978-1-4614-6867-7.
- 648 Eddelbuettel, D. and Balamuta, J. J. (2018). Extending extitR with extitC++: A Brief  
 649 Introduction to extitRcpp. *The American Statistician*, 72(1):28–36.
- 650 Eddelbuettel, D. and François, R. (2011). Rcpp: Seamless R and C++ Integration. *Journal  
 651 of Statistical Software*, 40(8):1–18.
- 652 Elliot, N. B., Cushman, S. A., Macdonald, D. W., and Loveridge, A. J. (2014). The Devil  
 653 is in the Dispersers: Predictions of Landscape Connectivity Change with Demography.  
 654 *Journal of Applied Ecology*, 51(5):1169–1178.
- 655 Fahrig, L. (2003). Effects of Habitat Fragmentation on Biodiversity. *Annual Review of  
 656 Ecology, Evolution, and Systematics*, 34(1):487–515.
- 657 Fattebert, J., Robinson, H. S., Balme, G., Slotow, R., and Hunter, L. (2015). Structural  
 658 Habitat Predicts Functional Dispersal Habitat of a Large Carnivore: How Leopards  
 659 Change Spots. *Ecological Applications*, 25(7):1911–1921.
- 660 Fieberg, J., Signer, J., Smith, B., and Avgar, T. (2021). A ‘How to’ Guide for Interpreting  
 661 Parameters in Habitat-Selection Analyses. *Journal of Animal Ecology*, 90(5):1027–1043.
- 662 Fortin, D., Beyer, H. L., Boyce, M. S., Smith, D. W., Duchesne, T., and Mao, J. S. (2005).  
 663 Wolves Influence Elk Movements: Behavior Shapes a Trophic Cascade in Yellowstone  
 664 National Park. *Ecology*, 86(5):1320–1330.
- 665 Fortin, D., Fortin, M.-E., Beyer, H. L., Duchesne, T., Courant, S., and Dancose, K. (2009).  
 666 Group-Size-Mediated Habitat Selection and Group Fusion–Fission Dynamics of Bison  
 667 under Predation Risk. *Ecology*, 90(9):2480–2490.
- 668 Frankham, R., Briscoe, D. A., and Ballou, J. D. (2002). *Introduction to Conservation  
 669 Genetics*. Cambridge University Press, Cambridge, UK.

- 670 Graves, T. A. and Waller, J. S. (2006). Understanding the Causes of Missed Global Positioning System Telemetry Fixes. *Journal of Wildlife Management*, 70(3):844–851.
- 672 Gustafson, E. J. and Gardner, R. H. (1996). The Effect of Landscape Heterogeneity on the Probability of Patch Colonization. *Ecology*, 77(1):94–107.
- 674 Hanski, I. (1999). *Metapopulation Ecology*. Oxford University Press.
- 675 Hauenstein, S., Fattebert, J., Grüebler, M. U., Naef-Daenzer, B., Pe'er, G., and Hartig, F. (2019). Calibrating an Individual-Based Movement Model to Predict Functional Connectivity for Little Owls. *Ecological Applications*, 29(4):e01873.
- 678 Hijmans, R. J. (2021). *terra: Spatial Data Analysis*. R package version 1.2-10.
- 679 Hodel, F. H. and Fieberg, J. R. (2022). Circular-Linear Copulae for Animal Movement Data. *Methods in Ecology and Evolution*, pages 2041–210X.13821.
- 681 Hofmann, D. D., Behr, D. M., McNutt, J. W., Ozgul, A., and Cozzi, G. (2021a). Bound within boundaries: Do protected areas cover movement corridors of their most mobile, protected species? *Journal of Applied Ecology*, 58(6):1133–1144. Publisher: Wiley Online Library.
- 685 Hofmann, D. D., Behr, D. M., McNutt, J. W., Ozgul, A., and Cozzi, G. (2021b). Data from: Bound within Boundaries: Do Protected Areas Cover Movement Corridors of their Most Mobile, Protected Species? Dryad Digital Repository. <https://doi:10.5061/dryad.dncjsxkzn>.
- 689 Kanagaraj, R., Wiegand, T., Kramer-Schadt, S., and Goyal, S. P. (2013). Using Individual-Based Movement Models to Assess Inter-Patch Connectivity for Large Carnivores in Fragmented Landscapes. *Biological Conservation*, 167:298 – 309.
- 692 Koen, E. L., Bowman, J., Sadowski, C., and Walpole, A. A. (2014). Landscape Connectivity for Wildlife: Development and Validation of Multispecies Linkage Maps. *Methods in Ecology and Evolution*, 5(7):626–633.
- 695 Koen, E. L., Garroway, C. J., Wilson, P. J., and Bowman, J. (2010). The Effect of Map Boundary on Estimates of Landscape Resistance to Animal Movement. *PLoS ONE*, 5(7):e11785.
- 698 Landguth, E. L., Hand, B. K., Glassy, J., Cushman, S. A., and Sawaya, M. A. (2012). UNICOR: A Species Connectivity and Corridor Network Simulator. *Ecography*, 35(1):9–14.
- 701 LaPoint, S., Gallery, P., Wikelski, M., and Kays, R. (2013). Animal Behavior, Cost-Based Corridor Models, and Real Corridors. *Landscape Ecology*, 28(8):1615–1630.
- 703 Latham, A. D. M., Latham, M. C., Boyce, M. S., and Boutin, S. (2011). Movement Responses by Wolves to Industrial Linear Features and Their Effect on Woodland Caribou in Northeastern Alberta. *Ecological Applications*, 21(8):2854–2865.
- 706 Leigh, K. A., Zenger, K. R., Tammen, I., and Raadsma, H. W. (2012). Loss of Genetic Diversity in an Outbreeding Species: Small Population Effects in the African Wild Dog (*Lycaon pictus*). *Conservation Genetics*, 13(3):767–777.
- 709 MacArthur, R. H. and Wilson, E. O. (2001). *The Theory of Island Biogeography*, volume 1. Princeton University Press, Princeton, New Jersey, USA.
- 711 Martensen, A. C., Saura, S., and Fortin, M. (2017). Spatio-Temporal Connectivity: Assessing the Amount of Reachable Habitat in Dynamic Landscapes. *Methods in Ecology and Evolution*, 8(10):1253–1264.
- 714 Masenga, E. H., Jackson, C. R., Mjingo, E. E., Jacobson, A., Riggio, J., Lyamuya, R. D., Fyumagwa, R. D., Borner, M., and Røskraft, E. (2016). Insights into Long-Distance Dispersal by African Wild Dogs in East Africa. *African Journal of Ecology*, 54(1):95–98.

- 717 McClintock, B. T., King, R., Thomas, L., Matthiopoulos, J., McConnell, B. J., and Morales,  
718 J. M. (2012). A General Discrete-Time Modeling Framework for Animal Movement Using  
719 Multistate Random Walks. *Ecological Monographs*, 82(3):335–349.
- 720 McClure, M. L., Hansen, A. J., and Inman, R. M. (2016). Connecting Models to Movements:  
721 Testing Connectivity Model Predictions against Empirical Migration and Dispersal Data.  
722 *Landscape Ecology*, 31(7):1419–1432.
- 723 McNutt, J. (1996). Sex-Biased Dispersal in African Wild Dogs (*Lycaon pictus*). *Animal  
724 Behaviour*, 52(6):1067–1077.
- 725 McRae, B. H. (2006). Isolation by Resistance. *Evolution*, 60(8):1551–1561.
- 726 McRae, B. H., Dickson, B. G., Keitt, T. H., and Shah, V. B. (2008). Using Circuit Theory to  
727 Model Connectivity in Ecology, Evolution, and Conservation. *Ecology*, 89(10):2712–2724.
- 728 Muff, S., Signer, J., and Fieberg, J. (2020). Accounting for Individual-Specific Variation in  
729 Habitat-Selection Studies: Efficient Estimation of Mixed-Effects Models Using Bayesian  
730 or Frequentist Computation. *Journal of Animal Ecology*, 89(1):80–92.
- 731 Osipova, L., Okello, M. M., Njumbi, S. J., Ngene, S., Western, D., Hayward, M. W., and  
732 Balkenhol, N. (2019). Using Step-Selection Functions to Model landscape Connectivity  
733 for African Elephants: Accounting for Variability across Individuals and Seasons. *Animal  
734 Conservation*, 22(1):35–48.
- 735 O'Neill, H. M. K., Durant, S. M., and Woodroffe, R. (2020). What Wild Dogs Want: Habitat  
736 Selection Differs across Life Stages and Orders of Selection in a Wide-Ranging Carnivore.  
737 *BMC Zoology*, 5(1).
- 738 Panzacchi, M., Van Moorter, B., Strand, O., Saerens, M., Kivimäki, I., St. Clair, C. C.,  
739 Herfindal, I., and Boitani, L. (2016). Predicting the Continuum Between Corridors and  
740 Barriers to Animal Movements Using Step Selection Functions and Randomized Shortest  
741 Paths. *Journal of Animal Ecology*, 85(1):32–42.
- 742 Perrin, N. and Mazalov, V. (2000). Local Competition, Inbreeding, and the Evolution of  
743 Sex-Biased Dispersal. *The American Naturalist*, 155(1):116–127.
- 744 Pinto, N. and Keitt, T. H. (2009). Beyond the Least-Cost Path: Evaluating Corridor  
745 Redundancy Using a Graph-Theoretic Approach. *Landscape Ecology*, 24(2):253–266.
- 746 Pomilia, M. A., McNutt, J. W., and Jordan, N. R. (2015). Ecological Predictors of African  
747 Wild Dog Ranging Patterns in Northern Botswana. *Journal of Mammalogy*, 96(6):1214–  
748 1223.
- 749 Potts, J. R., Bastille-Rousseau, G., Murray, D. L., Schaefer, J. A., and Lewis, M. A. (2013).  
750 Predicting local and non-local effects of resources on animal space use using a mechanistic  
751 step selection model. *Methods in Ecology and Evolution*, 5(3):253–262.
- 752 R Core Team (2020). *R: A Language and Environment for Statistical Computing*. R Foun-  
753 dation for Statistical Computing, Vienna, Austria.
- 754 Rudnick, D., Ryan, S., Beier, P., Cushman, S., Dieffenbach, F., Epps, C., Gerber, L., Hart-  
755 ter, J., Jenness, J., Kintsch, J., Merenlender, A., Perkl, R., Perziosi, D., and Trombulack,  
756 S. (2012). The Role of Landscape Connectivity in Planning and Implementing Conserva-  
757 tion and Restoration Priorities. *Issues in Ecology*.
- 758 Sawyer, S. C., Epps, C. W., and Brashares, J. S. (2011). Placing Linkages among Fragmented  
759 Habitats: Do Least-Cost Models Reflect How Animals Use Landscapes? *Journal of  
760 Applied Ecology*, 48(3):668–678.
- 761 Signer, J., Fieberg, J., and Avgar, T. (2017). Estimating Utilization Distributions from  
762 Fitted Step-Selection Functions. *Ecosphere*, 8(4):e01771.

- 763 Tischendorf, L. and Fahrig, L. (2000). On the Usage and Measurement of Landscape Con-  
764 nectivity. *Oikos*, 90(1):7–19.
- 765 Turchin, P. (1998). *Quantitative Analysis of Movement: Measuring and Modeling Population*  
766 *Redistribution in Plants and Animals*. Sinauer Associates, Sunderland, MA, USA.
- 767 Van der Meer, E., Fritz, H., Blinston, P., and Rasmussen, G. S. (2014). Ecological Trap in  
768 the Buffer Zone of a Protected Area: Effects of Indirect Anthropogenic Mortality on the  
769 African Wild Dog (*Lycaon pictus*). *Oryx*, 48(2):285–293.
- 770 Vasudev, D., Fletcher, R. J., Goswami, V. R., and Krishnadas, M. (2015). From Disper-  
771 sal Constraints to Landscape Connectivity: Lessons from Species Distribution Modeling.  
772 *Ecography*, 38(10):967–978.
- 773 Whittingham, M. J., Stephens, P. A., Bradbury, R. B., and Freckleton, R. P. (2006). Why Do  
774 We Still Use Stepwise Modelling in Ecology and Behaviour? *Journal of Animal Ecology*,  
775 75(5):1182–1189.
- 776 Wolski, P., Murray-Hudson, M., Thito, K., and Cassidy, L. (2017). Keeping it Simple:  
777 Monitoring Flood Extent in Large Data-Poor Wetlands Using MODIS SWIR Data. *In-*  
778 *ternational Journal of Applied Earth Observation and Geoinformation*, 57:224–234.
- 779 Woodroffe, R., Rabaiotti, D., Ngatia, D. K., Smallwood, T. R. C., Strelbel, S., and O'Neill,  
780 H. M. K. (2019). Dispersal Behaviour of African Wild Dogs in Kenya. *African Journal*  
781 *of Ecology*.
- 782 Woodroffe, R. and Sillero-Zubiri, C. (2012). *Lycaon pictus*. *The IUCN Red List of Threatened*  
783 *Species*, 2012:e. T12436A1671116.
- 784 Zeller, K. A., Wattles, D. W., Bauder, J. M., and DeStefano, S. (2020). Forecasting Seasonal  
785 Habitat Connectivity in a Developing Landscape. *Land*, 9(7):233.

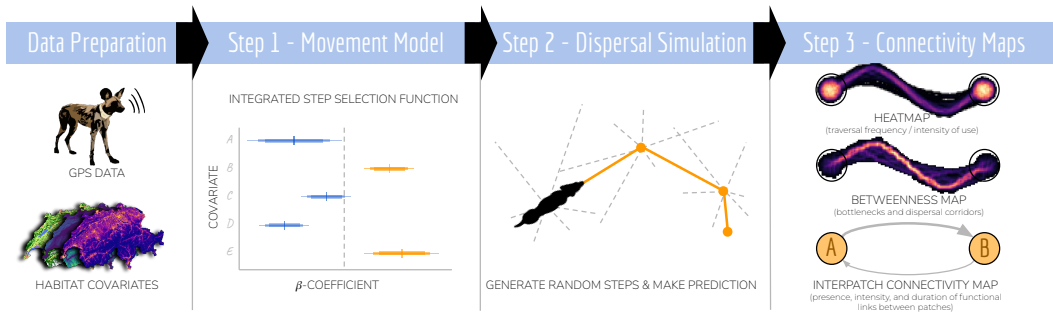


**Figure 1:** Flowchart of the simulation-based connectivity analysis. First, GPS data and habitat covariates must be collected. The combined data is then analyzed using an integrated step selection model (step 1). The parametrized model is then treated as an individual-based movement model and used to simulate dispersal trajectories (step 2). Ultimately, simulated trajectories are translated into a set of maps that are pertinent to landscape connectivity (step 3). This includes a heatmap, indicating the traversal frequency across each spatial unit of the study area, a betweenness map, highlighting movement corridors and bottlenecks, and, finally, an inter-patch connectivity map, where the frequency of connections and their average duration can be depicted.

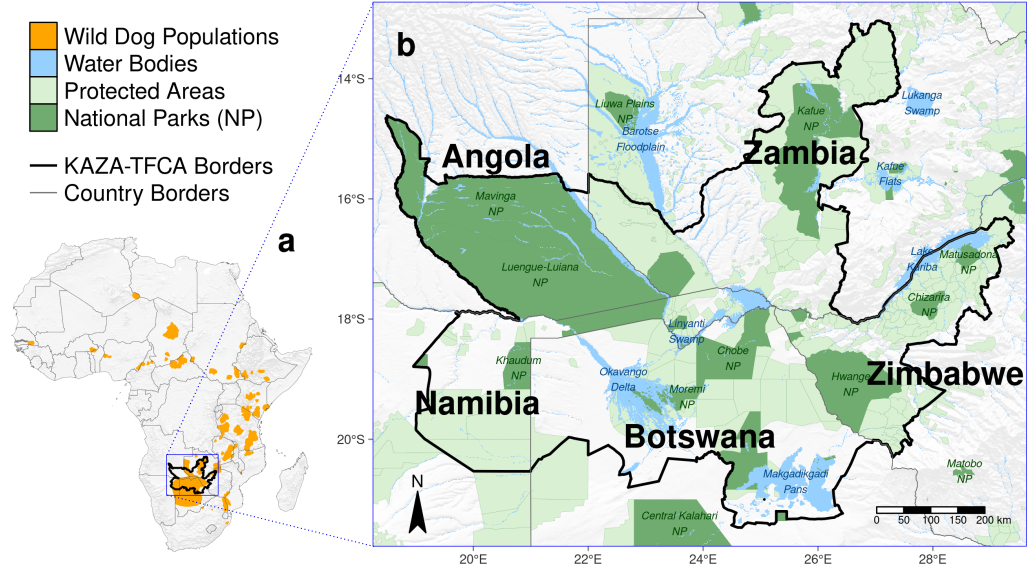


**Figure 2:** Illustration of the study area in southern Africa. (a) The study area was confined by a bounding box spanning the entire KAZA-TFCA which comprises parts of Angola, Namibia, Botswana, Zimbabwe, and Zambia. Data on remaining wild dog populations (orange) has been sourced from Woodroffe and Sillero-Zubiri (2012). (b) The KAZA-TFCA represents the world's largest terrestrial transfrontier conservation area and covers a total area of 520'000 km<sup>2</sup>. Its main purpose is to re-establish connectivity between already-existing NPs (dark green) and other protected areas (light green).

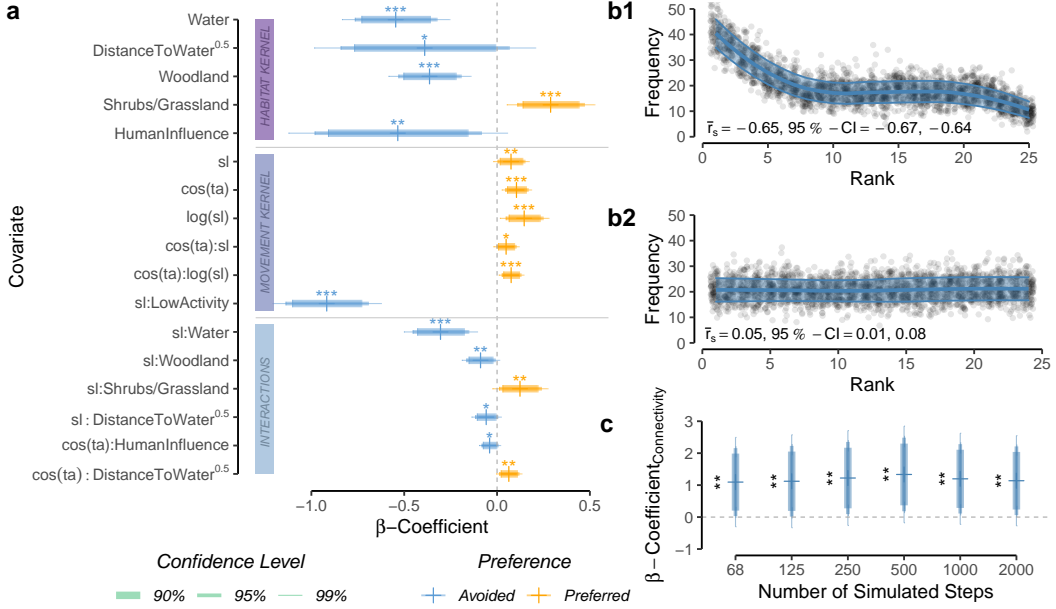


**Figure 3:** (a) Most parsimonious movement model for dispersing wild dogs. The model comprises a habitat kernel, a movement kernel, as well as their interactions. The horizontal line segments delineate the 90%, 95%, and 99% confidence-intervals for the respective  $\beta$ -coefficients. Significance codes: \*  $p < 0.10$ , \*\*  $p < 0.05$ , \*\*\*  $p < 0.01$ . (b) Results from the k-fold cross validation procedure. Subfigure b1 shows rank frequencies of realized steps according to model predictions with known preferences, whereas subfigure b2 shows rank frequencies of realized steps when assuming random preferences. The blue ribbon shows the prediction interval around a loess smoothing regression that we fitted to ease the interpretation of the plots. The significant correlation between rank and associated frequency in (b1) highlights that the most parsimonious model successfully outperformed a random guess (b2) and frequently assigned low ranks (i.e. high selection scores) to realized steps but only rarely high ranks (i.e. low selection scores). (c) Results from the PSF analysis using independent dispersal data show that dispersers preferably moved through areas where our heatmaps predicted high connectivity. Results are shown for heatmaps realized after 68, 125, 250, 500, and 2'000 simulated steps, respectively.

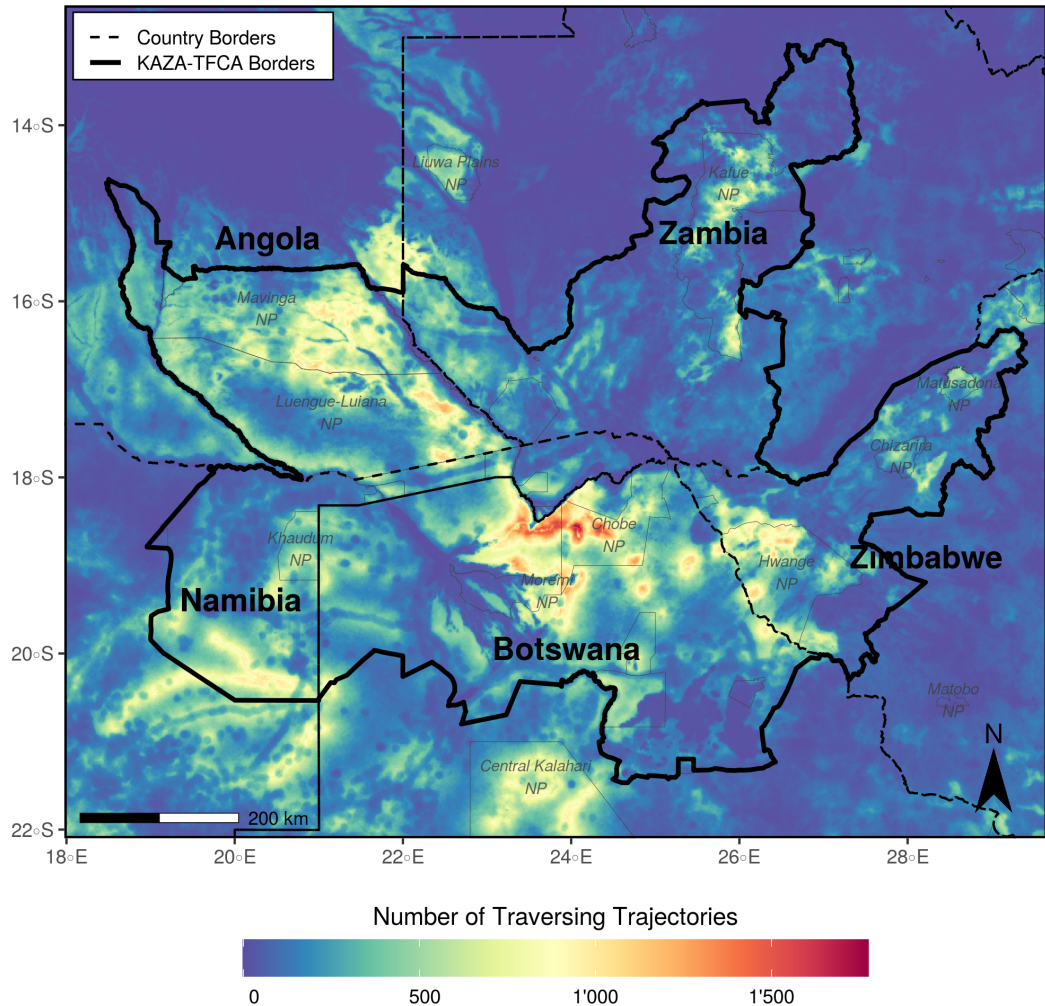


**Figure 4:** Heatmap showing traversal frequencies of 80'000 simulated dispersers moving 2'000 steps across the KAZA-TFCA. Simulations were based on an integrated step-selection model that we fitted to the movement data of dispersing African wild dogs. To generate the heatmap, we rasterized and tallied all simulated trajectories. Consequently, the map highlights areas that are frequently traversed. For spatial reference we plotted a few selected NPs (dark gray). Additional heatmaps showing the traversal frequency when individuals move fewer than 2'000 steps are provided in Figure S5.

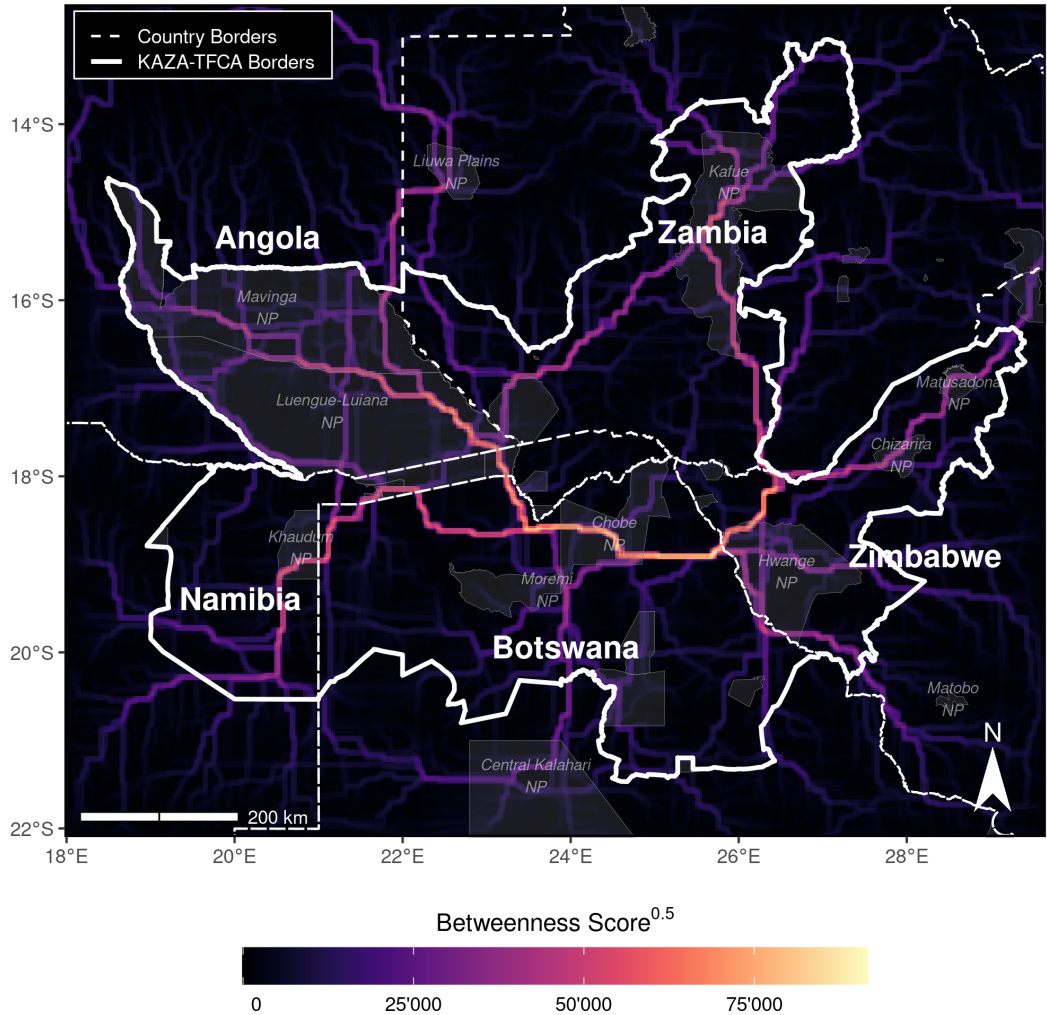


**Figure 5:** Map of betweenness scores, highlighting distinct dispersal corridors and potential bottlenecks across the extent of the KAZA-TFCA. Betweenness measures the number of shortest paths traversing through each node (raster-cell). Hence, a high betweenness score indicates that the respective area is exceptionally important for connecting different regions in the study area. The metric is therefore useful to pinpoint discrete movement corridors (Bastille-Rousseau et al., 2018). Note that we square-rooted betweenness scores to improve visibility of corridors with comparably low scores. Additional betweenness maps showing betweenness scores when individuals move fewer than 2'000 steps are provided in Figure S6.

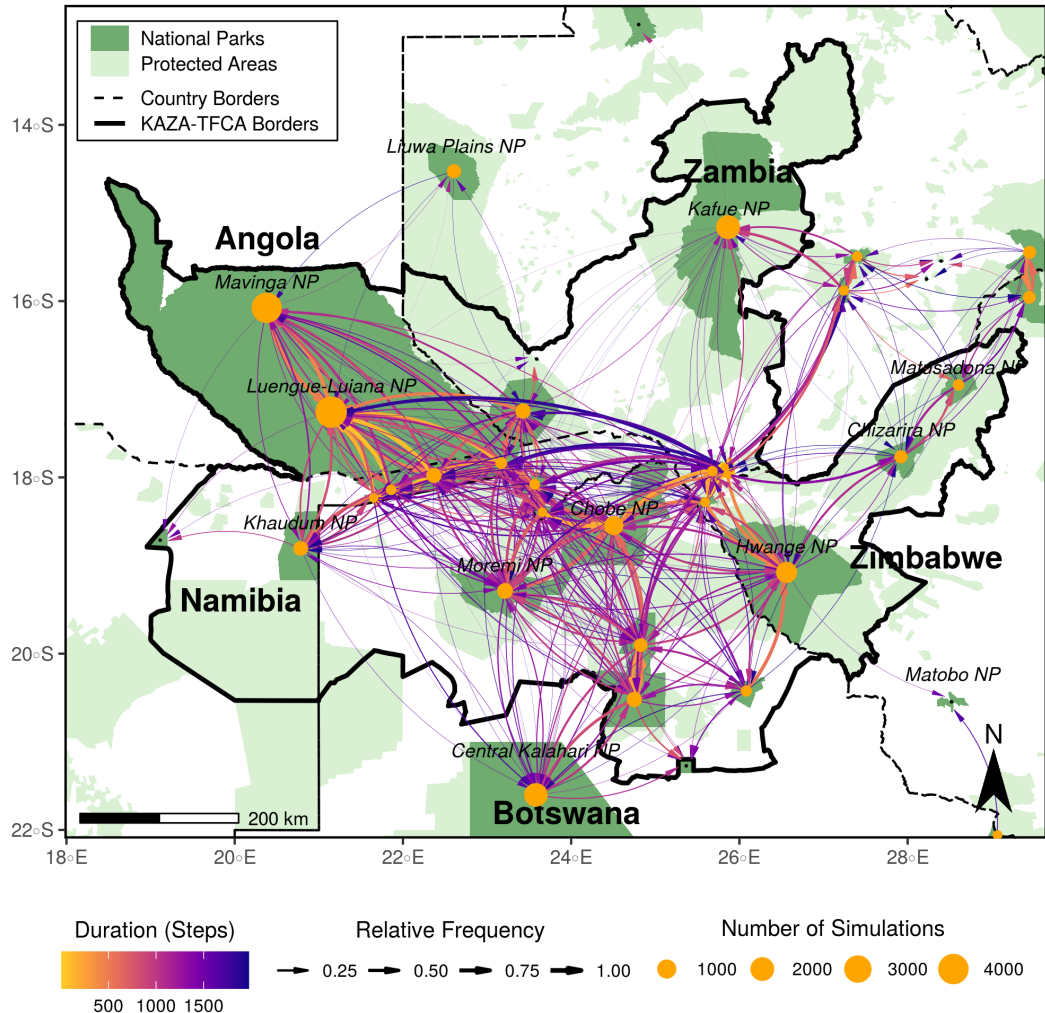


**Figure 6:** Map of inter-patch connectivity in relation to dispersal duration, highlighting connections between NPs (dark green). Yellow bubbles represent the center of the different NPs and are sized in relation to the number of simulated dispersers originating from each park. Black dots represent NPs that were smaller than  $700 \text{ km}^2$  and therefore were not used as source areas. Arrows between NPs illustrate between which NPs the simulated dispersers successfully moved and the color of each arrow shows the average number of steps (i.e. 4-hourly movements) that were necessary to realize those connections. Additionally, the line thickness indicates the relative number of dispersers originating from a NP that realized those connections.